Preparation of erbium activated yttrium orthovanadate-phosphate by chemical bath deposition.

M Mokoena[1*], KG Tshabalala[1], HC Swart[1], BF Dejene[2], MR Mhlongo[3], and S.J Motloung[1]

[1]Department of Physics, University of the Free State, P.O. Box 339, Bloemfontein/QwaQwa campus, 9300, South Africa
[2]Department of Chemical and Physical Science, Walter Sisulu University (Mthatha Campus**)**, Private Bag X 1, Mthatha, 5117

[3]Department of Physics, Sefako Makgatho Health Science University, Medunsa 0204, South Africa

Corresponding Author Email address: *tlousj@gmail.com* or *mokoenamosidi2@gmail.com*

Abstract
Erbium (Er^{3+}) activated yttrium orthovanadate-phosphate ($YV_{0.5}P_{0.5}O_4$) nanomaterials were prepared by chemical bath deposition. The concentration of Er^{3+} varied between 1 and 10 mol%. The structure, surface morphology, elemental composition and optical analysis were carried out by X-ray diffraction (XRD), scanning electron microscopy (SEM), energy-dispersive X-ray spectroscopy (EDS), and UV–vis spectroscopy (UV). XRD results showed that all the samples have a tetragonal zircon structure. SEM shows that the particles were in the nano-range and portrayed nanosphere shapes. The presence of all the elements forming $YV_{0.5}P_{0.5}O_4$: Er^{3+} was verified by EDS. Diffuse reflectance spectra (DRS) revealed a broad absorption band in the UV region which is attributed to the absorption of VO_4^{3-}. Other f→f transitions of Er^{3+} were also observed at 380, 407, 451, 489, 523, 546 and 654 nm and were attributed to $^4I_{15/2} - {}^4G_{11/2}$, $^4I_{15/2} - {}^4F_J$ (J= 3/2, 5/2, 7/2, 9/2), $^4I_{15/2} - {}^2H_{9/2,}$ $^2H_{11/2} - {}^4I_{15/2}$, and $^4S_{3/2} - {}^4I_{15/2}$ electronic transitions of Er^{3+}. Lastly, the estimated band gaps were found to be between 3.76 and 3.82 eV.
Keywords: Up-conversion; Nanophosphors; Rare earth; Optical properties

1. Introduction

In recent years, lanthanide (Ln^{3+})-activated up-conversion (UC) materials have become a topic of intense research due to their superior chemical and characteristic optical properties, such as their low optical background, excellent photostability, ease of manufacture, low toxicity, and high UC luminescence. Our world faces a serious energy issue. Fossil fuels are presently the main energy source, but they present challenges such as environmental pollution and the depletion of such fuels; hence there is a need for alternative renewable energy sources. Therefore, in this study, our focus was on synthesizing an UC luminescent material that can act as an UC layer when exposed to infra red light. Currently, rare-earth (RE) doped nanophosphors are considered superior optical materials to produce light-emitting materials. REs ions exhibit narrow emission and excitation bands due to an electronic transition from f-f, which is why they are widely used to generate luminescence. A wide range of applications can be achieved with rare-earth luminescence materials, including phosphors, display monitors, X-ray imaging, scintillators, lasers, and optical amplifiers [1]. A number of trivalent lanthanide ions, including $Er^{3+,}$ Tm^{3+}, Ho^{3+}, and Pr^{3+}, act as activators for UC processes due to their high energy levels. There have already been various UC phosphors developed, such as Ln^{3+} doped rare earth oxides, rare earth fluorides, alkaline earth metal fluorides, etc. [2]. A number of studies have been performed on the UC process for disordered matrices doped with the $4f^{11}$ lanthanide ion Er^{3+}. Er^{3+} is one of the rare-earth ions that is usually used as an important

activator in luminescent materials because it provides intermediate levels ($^4I_{11/2}$ and $^4I1_{3/2}$) with equally spaced and longer lifetime excited states, and this enables the conversion of infrared light to visible light [3]. The Er^{3+} ions may be excited either under down conversion or up conversion excitations to display green and white emission applications [4].

The most suitable host must have low phonon energy in order to engage non-radiative processes at a lower probability and then optimize the desired application performance. One of the newest developed phosphors are RE orthovanadates and orthophosphates with the general formula MNO_4, where M= Sc, Y, La, Gd or Lu and N= V or P. Among these orthovanadates or orthophosphates, yttrium orthovanadates (YVO_4) and orthophosphate (YPO_4) have been studied for a long time because they possess interesting properties, such as excellent thermal, mechanical, optical properties and chemical stability [5], [6]. Vanadate and phosphates can be combined to form orthovanadate-phosphate hosts, this orthovanadate-phosphate host can be achieved by partially replacing the V^{5+} ions with P^{5+} ions (or vice versa) in the YVO_4 (or YPO_4) system, usually resulting in a tetragonal structure [7]. Motloung et.al. [8] have illustrated that the stability and high-temperature luminescent properties of YVO_4 and YPO_4 can be enhanced by the orthovanadate-phosphate system.

In this study, Er^{3+} doped $YV_{0.5}P_{0.5}O_4$ powder materials were prepared by the chemical bath deposition (CBD) method. There are published reports on the synthesis of Er^{3+} doped $YV_{0.5}P_{0.5}O_4$ using various synthesis methods. However, to the best of our knowledge there are no reports on the synthesis of Er^{3+} doped $YV_{0.5}P_{0.5}O_4$ by CBD. The method, which is cheap and simple, is a low temperature technique which uses a solution that produces a crystal size that is often very small and homogeneous. The phase structures, morphologies, elemental, and optical properties of the $YV_{0.5}P_{0.5}O_4$: x% Er^{3+} samples were investigated in detail.

2. Experiment

Materials synthesis: Yttrium nitrate hexahydrate ($Y(NO_3)_3 \cdot (H_2O)_6$) (99.8% trace metal bases), ammonium metavanadate (NH_4VO_4) (P = 99%), ammonia (25% NH_3), erbium (III) acetate hydrate $C_6H_9ErO_6 \cdot H_2O$ (99.8% trace metal bases), ammonium dihydrogen phosphate ($NH_4H_2PO_4$) and deionized water were used throughout the experiment. All solvents and chemicals used were of analytical grade and purchased from Sigma Aldrich.$YV_{0.5}P_{0.5}O_4$:x% Er^{3+} (where x = 1, 3, 5, 7 and 10) phosphor- powders doped with Er^{3+} (x mol%) were prepared by chemical bath deposition at 80 ℃. In a typical preparation, 0.05M of $Y(NO_3)_3 \cdot (H_2O)_6$, 0.025M of NH_4VO_4, and 0.025 M $NH_4H_2PO_4$ solutions were prepared using deionized water under magnetic stirring. The solutions were stirred to allow homogenous mixing. The volume ratios (1:0,5:0,5) were then considered for each solution in the following order: 50 ml of $Y(NO_3)_3 \cdot (H_2O)_6$ was first added to the test tube placed in the water bath, followed by the addition of 50 ml of NH_4VO_4 solution and 50ml of $NH_4H_2PO_4$ solution, and lastly 50ml of (25% NH_3) solution was added drop-wise. The samples were prepared at five different concentrations of Er^{3+} (1, 3, 5, 7, and 10%). A white precipitate formed after the mixture was continuously stirred for several seconds. The reaction took place until 50ml of (25% NH_3) was used. The product was then allowed to stabilize and cool down overnight. Finally, the precipitates were collected, washed several times with ethanol and deionized water to remove the residue and desiccated in room temperature for a maximum of three days to ensure that powders were dried prior to characterization.

3. Results and discussion

X-ray diffraction

XRD patterns of the $YV_{0.5}P_{0.5}O_4$ nanophosphors doped with Er^{3+} at different concentrations are presented in Figure 1*a*. The XRD spectra show that the diffraction peaks matched well with the tetragonal zircon phase of YVO_4 (JCPDS file no. 17 − 0341). Figure 1*a* shows that the gradual increase of Er^{3+} from 1 to 10% mole did not influence the crystal structure. As the concentration of the dopant was increased, the XRD peak shows a slight shift to a higher diffraction degree (Fig 1*c*). This implies that the dopant ions are successfully and uniformly incorporated into the $YV_{0.5}P_{0.5}O_4$ host lattice [9]. This shift could be because of strains that are caused by the differences in ionic radii between vanadium (~ 0.54 Å), phosphorus (~ 0.35 Å) and the Er^{3+} (0.89 Å) [8]. To replace the trivalent yttrium ions with atomic radii of 0.9 Å with , the trivalent Er^{3+} ions with atomic radii of 0.89 Å are introduced in the $YV_{0.5}P_{0.5}O_4$: Er^{3+} system. Since both Y^{3+} and Er^{3+} ions have the same valency, Er^{3+} ion substitutions at the Y^{3+} site in $YV_{0.5}P_{0.5}O_4$ can lead to charge compensation issues [10]. According to the results, the phosphor powders were crystalline, and the diffraction peaks were found to be generally broad and this could be due to the small crystalline size of the material [5], [11]. No peaks are detected for any other impurities, demonstrating that pure phase products can be obtained when using the CBD synthesis method, and Er^{3+} can successfully replace Y^{3+}.

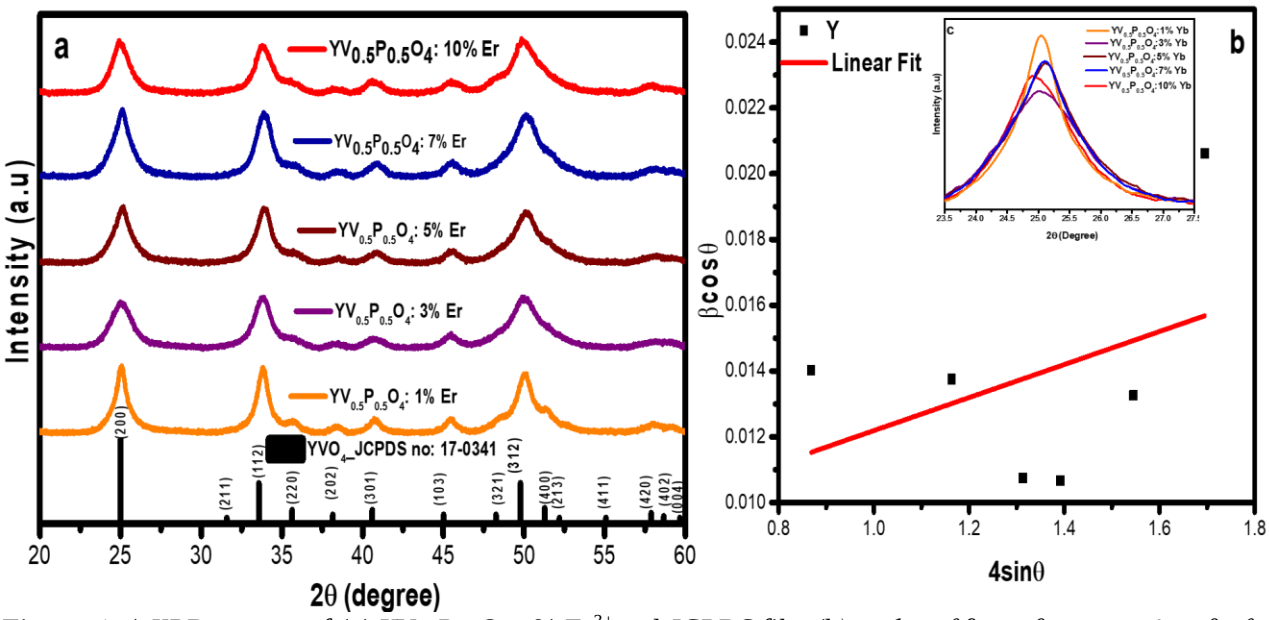

Figure. 1.a) XRD pattern of (a) $YV_{0.5}P_{0.5}O_4$:x% $Er^{3+}$and JCPDS file, (b) a plot of β cos θ against 4sin θ of $YV_{0.5}P_{0.5}O_4$:1% Er^{3+}, (c) XRD powder diffraction patterns of (200) for $YV_{0.5}P_{0.5}O_4$ doped with Er^{3+}.

Figure 1*c* shows an expanded view of the (200) diffraction peak for the samples synthesized at the different Er^{3+} concentrations. Williamson-Hall formula (equation 1) [12] was used to estimate the crystallite sizes and lattice strains.

$$B_{hkl}\cos\theta = 4\varepsilon\sin\theta + \frac{0.9\,\lambda}{D} \qquad 1$$

where D is the crystallite size, ε is the lattice strain, λ is the wavelength of the x-ray radiation (1.5406 Å), β is the full width at half maximum (FWHM) intensity, and θ is the diffraction angle at the peak position. The term (β cos θ) was plotted with respect to (4 sin θ) for the preferred orientation peaks of $YV_{0.5}P_{0.5}O_4$:1%Er^{3+} in figure 1*b*. The same procedure was used for different concentrations of Er^{3+}. The

results were found to be in a range of 19 to 17 nm and 0.00502 to 0.00973 for the crystallite sizes and lattice strains, respectively. The crystalline sizes were found to be fluctuating as Er^{3+} increased.

Scanning electron microscopy

The morphology of the prepared powder samples at various Er^{3+} mole concentrations is shown in figure 2. The morphology of the samples mainly consists of small primarily nanospheres structures, which show some conglomeration phenomena. Figure 2(*f and g*) shows low magnification, and it is observed that the product presents a bulk morphology conglomerating with an irregular quadrilateral shape with a uniform size. These results agree with XRD, which says that particles are tetragonal in shape. The mole concentration of Er^{3+} did not have influence on the morphology of the nanoparticles at low magnification. These irregular quadrilateral shape-like structures might be due to several nanospheres agglomeration. It is also noticed that low doping concentrations of Er^{3+} did not significantly affect morphology and the particle size did not change much as Er^{3+} concentration was increased.

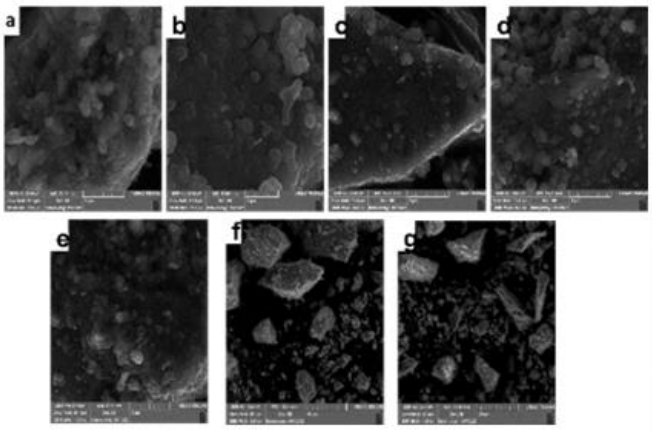

Figure 2: SEM images of (a,f) $YV_{0.5}P_{0.5}O_4$:1%Er^{3+} (b,g) $YV_{0.5}P_{0.5}O_4$:3% Er^{3+},c) $YV_{0.5}P_{0.5}O_4$:5% Er^{3+}, d) $YV_{0.5}P_{0.5}O_4$:7% Er^{3+},e) $YV_{0.5}P_{0.5}O_4$:10% Er^{3+}.

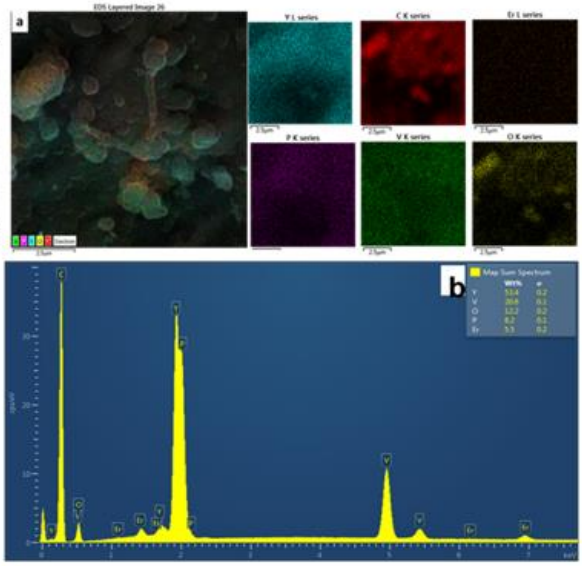

Figure 3(*a*) :The EDS elemental map of $YV_{0.5}P_{0.5}O_4$:5% Er^{3+}, *(b) The EDS spectrum of $YV_{0.5}P_{0.5}O_4$:5% Er^{3+}.*

Energy-dispersive X-ray spectroscopy

Electron diffraction X-ray spectroscopy (EDS) was used to analyze the composition of transition metals that are used to prepare $YV_{0.5}P_{0.5}O_4$:x% Er^{3+}. Elemental mapping of $YV_{0.5}P_{0.5}O_4$:5% Er^{3+}nanophosphor was observed through SEM to identify the composition of yttrium (Y), vanadium (V), phosphorus (P), oxygen (O), and erbium (Er) (Figure. 3*a*). The EDS spectrum (Fig. 3*b*) confirms the presence of the anticipated elements Y, V, P, O and Er in the $YV_{0.5}P_{0.5}O_4$:5% Er^{3+} samples. A carbon (C) peak was observed due to carbon tape being mounted to the sample when it was prepared for EDS measurements. In this study, the dopant was used at a low concentration thus, it was detected to be very small. No impurities were detected, which is in agreement with the XRD results. The same results were obtained for $YV_{0.5}P_{0.5}O_4$:1% Er^{3+}, $YV_{0.5}P_{0.5}O_4$:3% Er^{3+}, $YV_{0.5}P_{0.5}O_4$:7% Er^{3+}, and $YV_{0.5}P_{0.5}O_4$:10% Er^{3+} samples.

UV-Vis reflectance spectroscopy

$YV_{0.5}P_{0.5}O_4$ nanopowder was subjected to a UV-vis spectrometer to collect diffused reflectance spectrum and examine rare earth dopants' influence on its optical properties. The reflectance spectrum of $YV_{0.5}P_{0.5}O_4$ nanophosphors recorded as the function of wavelength in the wavelength range 200–800 nm prepared at various Er^{3+} molar concentrations is shown in figure 4*a*. It is evident that all the nanophosphors exhibited

a reflectance edge at about ~ 317 nm and this edge is attributed to the oxygen-to-vanadium atom charge transfer in the VO_4^{3-} units [8], [13]. In addition to the vanadate reflectance, the intrinsic f-f transitions of the Er^{3+} ion are noticed and are located at 380, 407, 451, 489, 523, 546 and 654 nm. These observed peaks can be attributed to the absorption of the Er^{3+} ion in the visible range and correspond to the electronic transition from $^4I_{15/2} - {}^4G_{11/2}$, $^4I_{15/2} - {}^4F_J$ (J= 3/2, 5/2, 7/2, 9/2), $^4I_{15/2} - {}^2H_{9/2,}$ $^2H_{11/2} - {}^4I_{15/2}$, and $^4S_{3/2} - {}^4I_{15/2}$ respectively [7], [13], [14]. Figure 4*a* shows that the reflectance intensity decreased as the molar concentration of Er^{3+} ions increased. The transformed Kubelka-Munk reflectance given in equation 2 [15] was used to obtain approximate band gap energies for the prepared powder samples.

$$\frac{K}{S} = \frac{(1-R)^2}{2R} \qquad 2$$

where R is a reflectance value, and K and S are the absorption and scattering coefficients. The bandgap, Eg, was calculated using the absorption edge wavelength for the interband transition in accordance with the equation below [16].

$$\alpha h\nu = A(h\nu - E_g)^2 \qquad 3$$

Where α, h*ν*, A, and E_g represent the light absorption coefficient, photon energy, proportional constant, and the bandgap value, respectively. These were represented in a transformed Kubelka-Munk reflectance plot represented in figure 7*b*. The band gap was estimated by extrapolating a straight line from the band edge to the intersection with h*ν* is the x-axis. From figure 4*b*, the band gaps of $YV_{0.5}P_{0.5}O_4$:1% Er^{3+}, $YV_{0.5}P_{0.5}O_4$:3% Er^{3+}, $YV_{0.5}P_{0.5}O_4$:5% Er^{3+}, $YV_{0.5}P_{0.5}O_4$:7% Er^{3+} and $YV_{0.5}P_{0.5}O_4$:10% Er^{3+} were extrapolated and found to be in the range of 3.78 to 3.82eV. The optical band gap energy of the doped $YV_{0.5}P_{0.5}O_4$ fluctuated as the molar concentrations of Er^{3+} was increased. This result is in accordance with the crystalline size, which fluctuated as the molar concentration of Er^{3+} increased, as confirmed by XRD analyses.

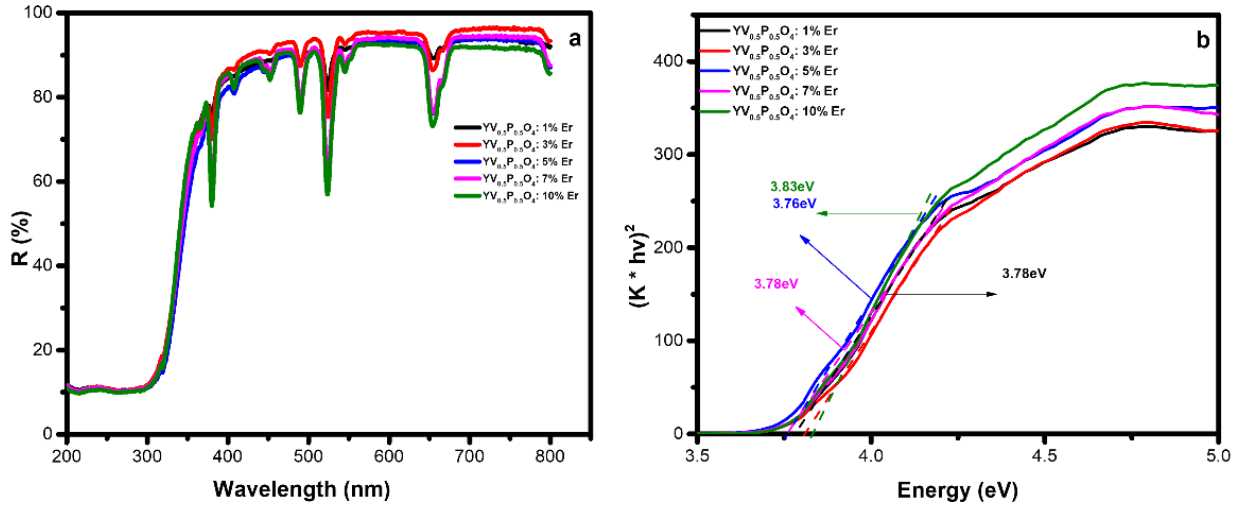

Figure 4. *(a) The diffuse reflectance spectra of* $YV_{0.5}P_{0.5}O_4$:x%Er^{3+}, *b) Transformed Kubelka−Munk reflectance of* $YV_{0.5}P_{0.5}O_4$:x%Er^{3+}.

Conclusion

In conclusion, Er^{3+} doped $YV_{0.5}P_{0.5}O_4$ phosphor powder have been synthesized by the CBD method for different concentrations of Er^{3+} ions and are characterized by XRD, SEM, EDS and UV. A successful introduction of Er^{3+} ions into the $YV_{0.5}P_{0.5}O_4$ lattice has been confirmed by XRD, SEM, and EDS measurements. As evidenced by XRD, the preparation of nanoparticles appeared to present a single phase of tetragonal zircon structure. The as-formed hybrid precursor materials present uniform small, primarily nanospheres like morphologies. The UV–vis reflectance spectra showed an intense Er^{3+} green peaks due to $^2H_{11/2} - {}^4I_{15/2}$, and $^4S_{3/2} - {}^4I_{15/2}$ transitions and other f→f transitions of Er^{3+} were also observed and were attributed $^4I_{15/2} - {}^4G_{11/2}$, $^4I_{15/2} - {}^4F_J$ (J= 3/2, 5/2, 7/2, 9/2), $^4I_{15/2} - {}^2H_{9/2,}$ electronic transitions of Er^{3+}. The band gap energies were calculated using a transformed reflectance Kubelka-Munk plot.

Acknowledgment
The authors gratefully thank the NRF, the Research Fund of the University of the Free State and the Department of Science and Technology (DST) of South Africa. This work is based on the research supported by the South African Research Chairs Initiative of the Department of Science and Technology and the National Research Foundation of South Africa.

References

[1] Sun Y, Liu H, Wang X, Kong X, and Zhang H 2006 *Chem. Mater* **18** 2726-2732

[2] Zhang C, Ma p, Li C, Li G, Huang S, Yang D, Shang M, Kang X and Lin J 2011 *J. Mater. Chem* **21** 717-723

[3] Liang Y, Chui P, Sun X, Zhao Y Cheng F, and Sun K 2013 *Journal of Alloys and Compounds* **552** 289–293

[4] Beltaif M, Koubaa T, Kallel T, Dammak M, Guidara K, and Khirouni K 2019 *Solid State Sciences* **90** 21–28

[5] Motloung S J, Tshabalala K G, and Ntwaeaborwa O M 2017 *Advanced Materials Letters* **8** 735–740

[6] Miao J, Wen Y, Wang W, Su J, Xu J, Zhong P and Rao W 2015 *Journal of Materials Science: Materials in Electronics* **26** 6178–6181

[7] Ayachi F, Saidi K, Chaabani W, and Dammak M 2021 *Journal of Luminescence 240*

[8] Motloung S J, Lephoto M A, Tshabalala K G, and Ntwaeaborwa O M 2018 *Physica B: Condensed Matter* **535** 211–215

[9] Gavrilović T V, Jovanović D J, Lojpur V, and Dramićanin M D 2014 *Scientific Reports 4*

[10] Thakur S and Gathania A K 2016 *Journal of Materials Science: Materials in Electronics* **27** 1988–1993

[11] Ansari A A and Labis J P 2012 *Materials Letters* **88** 152–155

[12] Mote V D, Purushotham Y, and Dole B N 2012 *Journal of Theoretical and Applied Physics* **6** 2251-7235

[13] Obregón S and Colón G 2015 *Chemical Engineering Journal* **262** 29–33

[14] Lee D Y, Lee M H, and Cho 2012 *Current Applied Physics* **12** 1229–1233.

[15] Motloung S V, Kumari P, Koao L F, Motaung T E, Hlatshwayo T T, and Mochane M. J *Materials Today Communications* **14** 294–301

[16] Borja-Urby R, Diaz-Torres L A, Salas P, Angeles-Chavez C, and Meza O 2011 *Materials Science and Engineering B: Solid-State Materials for Advanced Technology* **176** 1388–1392